

# Modelling Spectrum Assignment in a Two-Service Flexi-Grid Optical Link with Imprecise Continuous-Time Markov Chains

Cristina Rottondi\*, Alexander Erreygers†, Giacomo Verticale‡ and Jasper De Bock†

\*Dalle Molle Institute for Artificial Intelligence (IDSIA)

University of Lugano (USI) - University of Applied Science and Arts of Southern Switzerland (SUPSI)  
cristina.rotttondi@supsi.ch

†{SMACS Research Group, IDLab}, Ghent University, Belgium  
{alexander.erreygers, jasper.debock}@ugent.be

‡Dipartimento di Elettronica, Informazione e Bioingegneria, Politecnico di Milano, Italy  
giacomo.verticale@polimi.it

**Abstract**—The possibility of flexibly assigning spectrum resources with channels of different sizes greatly improves the spectral efficiency of optical networks. The drawback of this flexibility is the risk of spectrum fragmentation. We study this problem in the two-service scenario. Our first contribution consists of exact Markov models for different assignment policies. Since these exact models do not scale to large systems, we then extend an approximate, reduced-state model that is available in the literature. In addition, we introduce a Markov model that uses imprecise probabilities, which allows us to derive upper and lower bounds on blocking probabilities without needing to specify an assignment policy. The obtained imprecise Markov chain can be used to evaluate the precision of approximate reduced-state models as well as to provide policy-free performance bounds.

**Index Terms**—Two-Service Optical Link; Blocking Probability; Imprecise Continuous-Time Markov Chain;

## I. INTRODUCTION

Flexi-grid optical networks [1] have been envisioned as a novel paradigm to cope with the ever-growing Internet traffic: spectral resources are divided in small frequency slices (e.g. 12.5 GHz width, according to the ITU-T standard [2]) and groups of contiguous slices are adaptively assigned to different traffic requests (forming the so-called *superchannels*) according to their volume, the optical bandwidth of the transceivers in use and the adopted modulation format. Adjacent superchannels are separated by guardbands, constituted by one or multiple contiguous slices that are left unused. The advantages of flexi-grid networks have been quantified in terms of spectrum utilization reductions up to 30% with respect to traditional Wavelength Division Multiplexing (WDM) systems [3]. However, the flexi-grid approach requires more advanced and costly optical devices such as ROADMs with colorless/directionless/contentionless add/drop functionalities equipped with dedicated tunable filters supporting coherent detection [4]. Moreover, the flexible spectrum allocation techniques enabled by flexi-grid networks typically increase the spectrum fragmentation (i.e., the presence of groups of con-

tiguous slices that cannot be assigned to incoming traffic flows because the superchannel they could form would be too narrow to accommodate the demands). This issue is further increased by the spectrum continuity constraint, which requires that the same spectrum portion is allocated to a traffic flow along all the physical links it traverses. Therefore, several studies have been performed to identify fragmentation-aware spectrum allocation policies and to evaluate the corresponding blocking probabilities for traffic requests of different sizes [5]. Analytical models based on Markov Chains (MCs) have also been proposed [6]. Unfortunately, for exact solutions to realistic scenarios, these models require unaffordable computational resources due to the high number of chain states that are required to correctly capture the degrees of freedom offered by the flexible grid, thus introducing scalability limitations.

In order to alleviate the spectrum fragmentation issue and limit the costs of equipment installation without renouncing to the benefits of flexi-grid networks in terms of spectrum occupation reduction, alternative semi-flexible approaches have been proposed: traffic requests are grouped according to the number of slices required for transmission and requests belonging to the same group are placed along a dedicated fixed grid, with one edge of their superchannel anchored at a specific frequency [7]. Alternatively, a small set of predefined superchannel widths is defined and traffic flows are allocated in the smallest superchannel they fit in, at the price of leaving some spectrum slices unused [8]. Such scenarios allow for more scalable MC models: in [9] and [10], an approximate MC is proposed for quantifying blocking probabilities in a two-service semi-flexible optical link with a random spectrum allocation policy.

In this contribution, we first introduce an exact MC model for various spectrum allocation policies and then develop approximate versions based on the model in [9]. Finally, and most importantly, we compute bounds on the blocking probabilities that correspond to any arbitrary allocation policy.

To this aim, we adopt imprecise continuous-time MCs, a generalization of MCs obtained by applying the framework of imprecise probabilities [11], [12]. To the best of our knowledge, this is the first attempt to adopt such a mathematical tool in the context of optical networks modelling.

The remainder of this contribution is organized as follows. Section II presents an overview of the related scientific literature, whereas in Section III we provide some basic background on imprecise probabilities and their application to imprecise continuous-time MCs. Next, our proposed models are presented in Section IV and numerically assessed in Section V. Section VI concludes this contribution.

## II. RELATED WORK

A rich body of research work on flexi-grid optical networks has appeared in the last few years. The reader is referred to [13] and [14] for a thorough overview. More specifically, both the static and the dynamic Routing and Spectrum Assignment (RSA) problem in flexi-grid networks has been extensively addressed: [15] surveys the most relevant literature. In this paper, we focus on a single-link dynamic scenario, where the arrival and departure processes of traffic requests are random and requests are either accommodated in a spectrum portion of the link or rejected in real-time.

Different semi-flexible approaches have been proposed to mitigate the issue of spectrum fragmentation: in [8], the authors propose to partition the flexible grid in blocks of a fixed number of slices and to assign one block to each traffic request, regardless of its size, possibly leaving some unused slices within the block. If a single block is not sufficient to accommodate the whole traffic demand, multiple contiguous blocks are assigned to it. Alternatively, the authors of [16] propose to reserve a dedicated spectrum portion to high bit-rate signals, whereas in [7] each specific bit-rate signal uses its own dedicated fixed grid and starts from predefined anchor frequencies. In this paper, we adopt the latter approach.

A few studies investigate the unfairness of blocking probabilities in semi-flexible optical networks, under an assumption that traffic demands are categorized in two types according to their bit-rate (high or low, respectively): [9] proposes an approximate MC model for the calculation of blocking probabilities of the two types of traffic requests along a single optical link, assuming that spectrum assignment is performed randomly. This model has been refined in [10], [17], [18] to include spectrum portions exclusively reserved for each of the two connection types. In this paper, we generalize that model by means of an imprecise MC, which is an MC that allows for imprecise—i.e., partially specified—probabilities. In this way, we are able to provide guaranteed lower and upper bounds on the performance of *any* spectrum allocation policy.

A general introduction to the theory of imprecise probabilities can be found in [12]. This theory has been used to generalise both discrete-time and continuous-time MCs, the latter more recently than the former. A basic treatment of imprecise continuous-time MCs can be found in [19]–[21]. For their discrete-time version, see for example [22], [23].

## III. CONTINUOUS-TIME MARKOV CHAINS

A *continuous-time Markov chain* is a type of continuous-time stochastic process that is often used to model queueing systems. Since we will not consider the discrete-time version here, we can drop the prefix ‘continuous-time’ and can simply refer to them as Markov Chains (MCs). We start this section by recalling some well-established notation and terminology on MCs. After a brief introduction to imprecise probabilities, we then end by explaining the basics of imprecise MCs.

### A. Precise continuous-time Markov chains

We use  $(X_t)_{t \in \mathbb{R}_{\geq 0}}$  to denote a generic continuous-time stochastic process, where for all  $t \in \mathbb{R}_{\geq 0}$  the state  $X_t$  is a random variable that takes values  $x$  in the finite state space  $\mathcal{X}$ . Such a stochastic process  $(X_t)_{t \in \mathbb{R}_{\geq 0}}$  is called an MC if it satisfies the so-called *Markov property*, i.e., if

$$\begin{aligned} P(X_t = x_t | X_s = x_s, X_{t_1} = x_{t_1}, \dots, X_{t_n} = x_{t_n}) \\ = P(X_t = x_t | X_s = x_s) =: T_s^t(x_s, x_t), \end{aligned}$$

where  $n \geq 0$  is an integer and  $\{t_1, \dots, t_n, s, t\}$  is a strictly increasing sequence of non-negative time points. If we provide the state space  $\mathcal{X}$  with an ordering—which, from now, we assume to be the case—then the operator  $T_s^t$  can be interpreted as a matrix, the  $(x_s, x_t)$ -component of which is the transition probability  $P(X_t = x_t | X_s = x_s)$ . As a consequence of the Markov property, the transition matrices of an MC satisfy the following convenient property:

$$T_{t_1}^{t_n} = T_{t_1}^{t_2} T_{t_2}^{t_3} \dots T_{t_{n-1}}^{t_n}. \quad (1)$$

Moreover, if we use the ordering of  $\mathcal{X}$  to interpret a real-valued function  $f$  on  $\mathcal{X}$  as a column vector, then the  $x_s$ -component

$$[T_s^t f](x_s) := E(f(X_t) | X_s = x_s) \quad (2)$$

of the column vector  $T_s^t f$  is the expected value of  $f$  at time  $t$ , conditional on starting in the state  $x_s$  at time  $s$ . In particular, if we let  $\mathbb{I}_A$  be the indicator  $\mathbb{I}_A: \mathcal{X} \rightarrow \{0, 1\}$  of the event  $A \subseteq \mathcal{X}$ , defined by  $\mathbb{I}_A(x) := 1$  if  $x \in A$  and  $\mathbb{I}_A(x) := 0$  otherwise, then

$$[T_s^t \mathbb{I}_A](x_s) = P(X_t \in A | X_s = x_s). \quad (3)$$

An MC is called *stationary* if it satisfies  $T_t^{t+\Delta} = T_0^\Delta$  for all  $t, \Delta \in \mathbb{R}_{\geq 0}$ , in the sense that

$$P(X_{t+\Delta} = x | X_t = y) = P(X_\Delta = x | X_0 = y).$$

It is well-known that for any stationary MC, there exists a unique matrix  $Q$  such that  $T_t^{t+\Delta} = e^{\Delta Q}$ , where  $e^{\Delta Q}$  denotes the matrix exponential of  $\Delta Q$ . This matrix  $Q$  is called the *transition rate matrix* of the MC because, for all  $x, y \in \mathcal{X}$  such that  $x \neq y$ , and for sufficiently small  $\Delta \in \mathbb{R}_{\geq 0}$ ,

$$P(X_{t+\Delta} = x | X_t = y) \approx \Delta Q(x, y). \quad (4)$$

and

$$P(X_{t+\Delta} = x | X_t = x) \approx 1 + \Delta Q(x, x), \quad (5)$$

with  $Q(x, x) = -\sum_{y \neq x} Q(x, y)$ . In practice, a rate matrix  $Q$  is specified by providing numerical values for its non-zero rates, that is, for the non-zero off-diagonal elements. For example, if for some  $x \neq y$ , we say that the transition from  $x$  to  $y$  occurs with rate  $\lambda$ , this means that  $Q(x, y) = \lambda$ .

By combining (4) and (5), we find that  $T_t^{t+\Delta}$  can be approximated by  $(I + \Delta Q)$ , and therefore, it follows from (1) that

$$T_s^t = \lim_{n \rightarrow \infty} \left( I + \frac{t-s}{n} Q \right)^n. \quad (6)$$

Throughout this contribution, we are interested in probabilities of the form  $\lim_{t \rightarrow \infty} \mathbb{P}(X_t \in A | X_0 = x_0)$ , where  $A \subseteq \mathcal{X}$  and  $x_0 \in \mathcal{X}$ . If this probability does not depend on the initial state  $x_0$ , then we call it the limit probability of the event  $A$  and denote it with  $\pi_A$ . If every event  $A \subseteq \mathcal{X}$  has such a limit probability  $\pi_A$ , the MC is called *ergodic*. In practice, checking ergodicity does not require us to actually compute these limit probabilities. There are several well-known equivalent conditions that are easier to verify.

Provided that the MC is ergodic,  $\pi_A$  can be computed in two ways. On the one hand, (3) and (6) imply that

$$\pi_A = \lim_{t \rightarrow \infty} \lim_{n \rightarrow \infty} \left[ \left( I + \frac{t}{n} Q \right)^n \mathbb{I}_A \right] (x_0),$$

which allows us to compute  $\pi_A$  by choosing  $t$  and  $n$  sufficiently large. On the other hand, it is well known that for an ergodic MC the *limit distribution*  $\pi$ —when interpreted as a row vector whose components are the limit probabilities  $\pi_x$  of the states—is the unique probability mass function on  $\mathcal{X}$  that satisfies  $\pi Q = 0$ . Solving this linear system provides us with  $\pi$ , and  $\pi_A$  is then given by  $\pi_A = \sum_{x \in A} \pi_x$ .

### B. Imprecise probabilities

Whenever it is impossible or impractical to provide, obtain or compute exact values for the probability of some event, or the expectation of some function, the theory of imprecise probabilities allows for these quantities to be described ‘imprecisely’, using lower and upper bounds. For a detailed treatment of this theory, the interested reader is referred to [11] and [12]. For our present purposes, and in the context of stochastic processes, it suffices to understand the following basic concepts.

Mathematically, the most important notion is that of a conditional lower expectation, which is simply a lower bound on a conditional expectation. More formally, for any  $s, t \in \mathbb{R}_{\geq 0}$  such that  $t \geq s$ , any  $x_s \in \mathcal{X}$  and any function  $f: \mathcal{X} \rightarrow \mathbb{R}$ , the lower expectation of  $f$  at time  $t$ , conditional on  $X_s = x_s$ , is

$$\underline{\mathbb{E}}(f(X_t) | X_s = x_s) := \min_{\mathbb{E} \in \mathcal{E}} \mathbb{E}(f(X_t) | X_s = x_s),$$

where  $\mathcal{E}$  is the set of conditional expectations that corresponds to some set of stochastic processes  $\mathbb{P}$ —see Section III-C for a concrete example of such a set of processes  $\mathbb{P}$ .

The reason why we can focus on lower expectations, and not on upper expectations or lower/upper probabilities, is because the latter can all be obtained as special cases. On the one hand,

upper expectations are conjugate to lower expectations, in the sense that

$$\overline{\mathbb{E}}(f(X_t) | X_s = x_s) = -\underline{\mathbb{E}}(-f(X_t) | X_s = x_s). \quad (7)$$

On the other hand, lower and upper probabilities are special cases of lower and upper expectations, in the sense that for any event  $A \subseteq \mathcal{X}$ :

$$\underline{\mathbb{P}}(X_t \in A | X_s = x_s) = \underline{\mathbb{E}}(\mathbb{I}_A(X_t) | X_s = x_s), \quad (8)$$

and

$$\overline{\mathbb{P}}(X_t \in A | X_s = x_s) = \overline{\mathbb{E}}(\mathbb{I}_A(X_t) | X_s = x_s). \quad (9)$$

Lower and upper probabilities are also conjugate, in the sense that  $\overline{\mathbb{P}}(X_t \in A | X_s = x_s) = 1 - \underline{\mathbb{P}}(X_t \notin A | X_s = x_s)$ .

### C. Imprecise continuous-time Markov chains

Recently, several authors have applied the theory of imprecise probabilities to develop the notion of an imprecise continuous-time Markov chain, which we will here abbreviate as ‘imprecise MC’ [19], [20], [24]. Instead of a single precisely specified transition rate matrix  $Q$ , an imprecise MC considers a (closed and convex) set  $\mathcal{Q}$  of transition rate matrices. In practice, this is typically useful in cases where the values of the transition rates  $Q(x, y)$  cannot be determined exactly, as will for example be the case in Section IV-C further on.

More formally, instead of a single stationary MC, an imprecise MC considers the set  $\mathbb{P}_{\mathcal{Q}}$  of all MCs that are consistent with  $\mathcal{Q}$ , in the sense that at every point in time  $t \geq 0$ , and for  $\Delta \in \mathbb{R}_{\geq 0}$  sufficiently small, the transition matrix  $T_t^{t+\Delta}$  is approximately equal to  $I + \Delta Q_t$ , for some  $Q_t \in \mathcal{Q}$ . Note that the Markov chains in this set  $\mathbb{P}_{\mathcal{Q}}$  are not assumed to be stationary, in the sense that  $Q_t$  is not required to be constant. The only thing that is assumed about  $Q_t$  is that it is an—unknown—function of time that takes values in  $\mathcal{Q}$ .

As we consider a set of MCs, the transition matrices  $T_s^t$  are no longer uniquely known, as was the case for precise MCs. Instead, an imprecise MC is characterised by a lower transition operator  $\underline{T}_s^t$ . Analogous to (2), for any  $f: \mathcal{X} \rightarrow \mathbb{R}$  and any  $s, t \in \mathbb{R}_{\geq 0}$  such that  $t \geq s$ , the vector  $\underline{T}_s^t f$  is defined by

$$[\underline{T}_s^t f](x_s) := \underline{\mathbb{E}}(f(X_t) | X_s = x_s) \text{ for all } x_s \in \mathcal{X}, \quad (10)$$

where  $\underline{\mathbb{E}}(f(X_t) | X_s = x_s)$  is the minimum of the conditional expectations that are induced by the set of consistent processes  $\mathbb{P}_{\mathcal{Q}}$ . Of course, determining the set of all consistent processes in  $\mathbb{P}_{\mathcal{Q}}$  explicitly and then computing the minimum of the corresponding expectations is infeasible, if not impossible. However, fortunately, this is not necessary because the lower transition operator  $\underline{T}_s^t$  can often also be characterised by

$$\underline{T}_s^t = \lim_{n \rightarrow \infty} \left( I + \frac{t-s}{n} \underline{Q} \right)^n, \quad (11)$$

where  $\underline{Q}$  is the so-called *lower transition rate operator* of  $\mathcal{Q}$ , which transforms any real-valued function  $f$  on  $\mathcal{X}$  into a new function  $\underline{Q}f: \mathcal{X} \rightarrow \mathbb{R}$ , defined by

$$[\underline{Q}f](x) := \min \{ [Qf](x) : Q \in \mathcal{Q} \} \text{ for all } x \in \mathcal{X}. \quad (12)$$

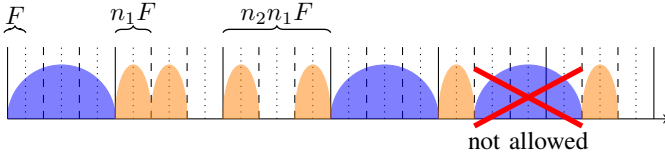


Fig. 1: Example of a semi-flexible optical grid with  $n_1 = 2$ ,  $n_2 = 3$  and  $S = 36$ .

As proved in [24], a sufficient condition for this to be possible is that  $\mathcal{Q}$  has separately specified rows, which basically means that for every  $f: \mathcal{X} \rightarrow \mathbb{R}$ , there is some  $Q \in \mathcal{Q}$  such that  $[Qf](x) = [Qf](x)$  for all  $x \in \mathcal{X}$ .

Now recall from Section III-A that in this contribution, for precise MCs, we are interested in the value of  $P(X_t \in A | X_0 = x_0)$  as  $t$  approaches infinity. Similarly, for imprecise MCs, we are interested in providing lower and upper bounds on this value as  $t$  approaches infinity, that is, we are interested in

$$\lim_{t \rightarrow \infty} \underline{P}(X_t \in A | X_0 = x_0) \quad \text{and} \quad \lim_{t \rightarrow \infty} \overline{P}(X_t \in A | X_0 = x_0).$$

As shown in [24], these limits always exist. If they furthermore do not depend on  $x_0 \in \mathcal{X}$ , then we call them the lower and upper limit probability of  $A$ , and denote them by  $\underline{\pi}_A$  and  $\overline{\pi}_A$ , respectively. Ergodicity is again a sufficient condition for the existence of  $\underline{\pi}_A$  and  $\overline{\pi}_A$ . For imprecise MCs, a definition for ergodicity and a simple method for checking whether it is verified can be found in [24].

Provided that the imprecise MC is ergodic and that  $\mathcal{Q}$  has separately specified rows, it follows from (7)–(11) that

$$\underline{\pi}_A = \lim_{t \rightarrow \infty} \lim_{n \rightarrow \infty} \left[ \left( I + \frac{t}{n} \underline{Q} \right)^n \mathbb{I}_A \right] (x_0)$$

and

$$\overline{\pi}_A = - \lim_{t \rightarrow \infty} \lim_{n \rightarrow \infty} \left[ \left( I + \frac{t}{n} \overline{Q} \right)^n (-\mathbb{I}_A) \right] (x_0),$$

which allows us to compute them both by choosing  $t$  and  $n$  sufficiently large.

#### IV. THE PROPOSED MARKOV CHAIN MODELS

This section provides a detailed description of the specific Markov chain models that we use. On the one hand, in Section IV-B, we introduce an exact MC that is able to model various spectrum assignment policies, but which does not scale to realistic scenarios. On the other hand, in Section IV-C, we provide models that do scale, at the cost of being approximate, and then use imprecise MCs to provide guaranteed bounds on these approximations. We start in Section IV-A by introducing some assumptions that are common to both types of models.

##### A. General Assumptions

We consider a single optical fibre link with overall spectrum availability of  $T$ . The spectrum is partitioned in slices of width  $F$ , for a total number of  $S = T/F$  slots. For the sake of easiness, we assume that  $T$  is an integer multiple of  $F$ . Slices are sequentially numbered from 1 to  $S$ .

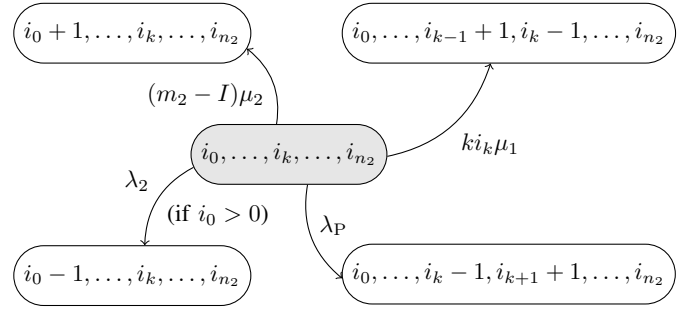


Fig. 2: State transition diagram of the proposed precise and exact Markov chain

Traffic requests of two different sizes are generated according to a Poisson random process with arrival rate  $\lambda_1$  (respectively  $\lambda_2$ ) and cease after a holding time with negative exponential distribution and average service time  $1/\mu_1$  (respectively  $1/\mu_2$ ). Traffic demands of type 1 require  $n_1 \geq 1$  slices, whereas demands of type 2 require  $n_2 \times n_1$  slices.

As depicted in Fig. 1, we consider two overlapping grids of coarser granularity. The first predefines a sequence of adjacent superchannels of width  $n_1 \times F$ : the first superchannel includes slices  $1, \dots, n_1$ , the second comprises slices  $n_1 + 1, \dots, 2n_1$ , and so on. Similarly, the second grid defines a sequence of adjacent superchannels of width  $n_2 \times n_1 \times F$ . The number of superchannels of size  $n_1 \times F$  is thus  $m_1 = S/n_1$ , whereas the number of superchannel of size  $n_2 \times n_1 \times F$  is  $m_2 = m_1/n_2$ . As before, for the sake of easiness, we assume that  $S$  is an integer multiple of  $n_1 \times n_2$ .

A type 1 request must be assigned to a free superchannel of width  $n_1 \times F$ , whereas a type 2 request must be placed in a free superchannel of width  $n_2 \times n_1 \times F$ . If no superchannel of the required size is available, the traffic request is blocked.

##### B. A Precise and Exact MC Model

Let  $(i_0, i_1, \dots, i_{n_2})$  be the state description of the MC, where  $i_k$  counts the number of type 2 superchannels occupied with  $k$  type 1 requests and no type 2 requests. Let  $I$  be defined as  $I = \sum_{k=0}^{n_2} i_k$ . Then  $m_2 - I$  is the number of type 2 superchannels that are occupied by a type 2 request. To ensure feasibility, it must hold that  $I \leq m_2$  and that  $i_k \geq 0$  for all  $k$  in  $[0, n_2]$ . Note that  $i_0$  counts the number of empty type 2 superchannels, whereas  $R = \sum_{k=0}^{n_2-1} i_k(n_2 - k)$  is the total number of free type 1 superchannels. If  $i_0 = 0$  and a type 2 request arrives, it must be blocked. However, a type 1 request can then still be allocated in an unused type 1 superchannel as long as  $R > 0$ . The total number of states of the chain exhibits an  $\mathcal{O}(m_2^{n_2})$  dependency on the total number of type 2 superchannels and on the number of type 1 superchannels contained in a type 2 superchannel.

As reported in Fig. 2, when a type 2 request arrives and finds an available type 2 superchannel (i.e.,  $i_0 > 0$ ), the following transition takes place with rate  $\lambda_2$ :  $(i_0, i_1, \dots, i_{n_2}) \rightarrow (i_0 - 1, i_1, \dots, i_{n_2})$ . Conversely, when a type 2 request departs after expiration of its holding time, the following transition

occurs:  $(i_0, i_1, \dots, i_{n_2}) \rightarrow (i_0 + 1, i_1, \dots, i_{n_2})$ . The rate of this transition is  $(m_2 - I)\mu_2$ .

Similarly, when a type 1 request departs, the state transition  $(i_0, \dots, i_k, \dots, i_{n_2}) \rightarrow (i_0, \dots, i_{k-1} + 1, i_k - 1, \dots, i_{n_2})$  occurs for all  $k$  in  $[1, n_1]$  with rate  $k i_k \mu_1$ . The state transition rate  $\lambda_P$  due to the arrival of type 1 requests depends on the adopted spectrum allocation policy  $P$ . This model can implement any policy that does not depend on the specific ordering of the type 1 superchannels allocated along the grid, but only on the number of type 1 superchannels in use within each type 2 superchannel. As exemplificative cases, here we report on three such policies.

If we adopt a Random spectrum Assignment policy (RA), then a new type 1 request is placed in any free superchannel of type 1 with equal probability. Therefore, the state transition  $(i_0, \dots, i_k, \dots, i_{n_2}) \rightarrow (i_0, \dots, i_k - 1, i_{k+1} + 1, \dots, i_{n_2})$  occurs for all  $k$  in  $[0, n_2 - 1]$  with rate  $\lambda_{RA} = \lambda_1 i_k (n_2 - k)^{1/R}$ , provided that  $R > 0$ . If  $R = 0$ , the request is rejected (i.e.,  $\lambda_{RA} = 0$ ).

Alternatively, if we adopt a policy that assigns the incoming type 1 request to the partially occupied type 2 superchannel that contains either the lowest number of type 1 superchannels already assigned (Least-Filled, LF) or the highest number of type 1 superchannels already assigned (Most-Filled, MF), we obtain the following transitions. As before, if  $R = 0$ , the request is rejected (i.e.,  $\lambda_{LM} = \lambda_{MF} = 0$ ). If  $R > 0$ , the state transition  $(i_0, \dots, i_{k_P}, \dots, i_{n_2}) \rightarrow (i_0, \dots, i_{k_P} - 1, i_{k_P+1} + 1, \dots, i_{n_2})$  occurs with rate  $\lambda_{LF} = \lambda_{MF} = \lambda_1$ , where  $k_P$  depends on the policy  $P$ . If there exists at least one superchannel of type 2 partially occupied by one or more type 1 requests (i.e., if  $\exists k \in [1, n_2 - 1]: i_k > 0$ ), then  $k_{LF} = \min\{k \in [1, n_2 - 1]: i_k > 0\}$  and  $k_{MF} = \max\{k \in [1, n_2 - 1]: i_k > 0\}$ . Otherwise, that is, if all the type 2 superchannels are either completely free or completely occupied (i.e.,  $i_k = 0$  for all  $k \in [1, n_2 - 1]$ ), then  $k_{LF} = k_{MF} = 0$ .

For each of the three spectrum assignment policies that we consider, the rates that were specified above determine a unique transition rate matrix  $Q$ . These transition rate matrices can furthermore be shown to be ergodic, and therefore, for every event  $A \subseteq \mathcal{X}$ , they each determine a unique limit probability  $\pi_A$ , which can be computed using the methods in Section III-A. The limit blocking probability BP1 experienced by type 1 traffic requests corresponds to choosing  $A = \{(i_0, \dots, i_{n_2}) \in \mathcal{X}: R = 0\}$ , whereas the limit blocking probability BP2 experienced by type 2 traffic requests is obtained by choosing  $A = \{(i_0, \dots, i_{n_2}) \in \mathcal{X}: i_0 = 0\}$ .

### C. An Imprecise and Scalable MC Model

The drawback of the model in Section IV-B is its limited scalability, which is due to the  $\mathcal{O}(m_2^{n_2})$  dependency on the superchannel sizes. In order to remedy this problem, we now present an alternative model that adopts the more compact—though less informative—state representation proposed in [9], thereby making it more scalable. This time, the state is described by the triplet  $(i, j, e)$ , where  $0 \leq i \leq m_1$  (resp.  $0 \leq j \leq m_2$ ) counts the number of type 1 (resp. type 2)

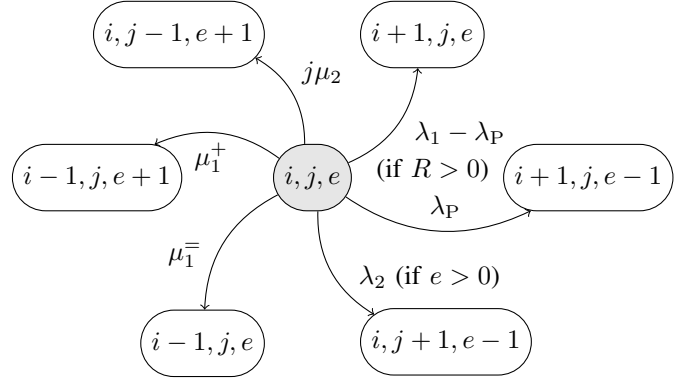


Fig. 3: State transition diagram of the precise but approximate Markov chain and of the proposed imprecise and scalable Markov chain

requests currently allocated, and  $0 \leq e \leq m_2$  counts the number of free superchannels of type 2. To ensure feasibility, it must hold that  $m_2 \leq i + j + e$  and  $i + (j + e)n_2 \leq m_1$ . The total number of states of the chain exhibits an  $\mathcal{O}(m_1 m_2^2)$  dependency on the total number of type 1 and type 2 superchannels.

As depicted in Fig. 3, when a type 2 request arrives and finds an available type 2 superchannel (i.e.,  $e > 0$ ), the following transition takes place with rate  $\lambda_2$ :  $(i, j, e) \rightarrow (i, j + 1, e - 1)$ . Conversely, when a type 2 request departs after expiration of its holding time, the following transition occurs:  $(i, j, e) \rightarrow (i, j - 1, e + 1)$ . The rate of this transition is equal to  $j\mu_2$ .

When a type 1 request departs, two transitions can occur:  $(i, j, e) \rightarrow (i - 1, j, e)$  or  $(i, j, e) \rightarrow (i - 1, j, e + 1)$ , the rates of which we will denote by  $\mu_1^-$  and  $\mu_1^+$ , respectively. The second transition corresponds to a type 1 request that is the only allocated type 1 request in its type 2 superchannel, whereas the first transition corresponds to a type 1 requests that shares its type 2 superchannel with other type 1 requests. If  $i = m_2 - j - e$ , then  $\mu_1^- = 0$  and  $\mu_1^+ = i\mu_1$  (i.e., a departure will always free a superchannel of type 2), whereas if  $i \geq n_2(m_2 - j - e - 1) + 2$  then  $\mu_1^- = i\mu_1$  and  $\mu_1^+ = 0$  (i.e., a departure will never free a superchannel of type 2). Unfortunately, in the remaining cases (i.e., if  $m_2 - j - e < i < n_2(m_2 - j - e - 1) + 2$ ), since the state representation is not sufficiently informative to capture the distribution of the allocated type 1 requests across the type 1 superchannels, it is not possible to determine  $\mu_1^-$  and  $\mu_1^+$  as a function of  $(i, j, e)$ , and they are then both unknown functions of  $(i, j, e, t)$ , where  $t$  is the time of the transition. All we can say for sure is that they are non-negative, that their sum is equal to  $i\mu_1$  and that

$$\mu_1^+(i, j, e, t) \in [i_{\min}(i, j, e)\mu_1, i_{\max}(i, j, e)\mu_1], \quad (13)$$

where  $i_{\min}(i, j, e) := \max\{0, 2(m_2 - j - e) - i\}$  is the minimum number of allocated type 1 requests that are alone in their type 2 superchannel and

$$i_{\max}(i, j, e) := \min \left\{ m_2 - j - e, \left\lfloor \frac{n_2(m_2 - j - e) - i}{n_2 - 1} \right\rfloor \right\}$$

is the maximum number of such type 1 requests.

In order to deal with this indeterminacy, the authors of [9] replace (13) with an approximate estimate for  $\mu_1^+(i, j, e, t)$ , which is based on an assumption that all the possible situations—that is, all possible distributions of type 1 requests—that are represented by the state  $(i, j, e)$  are equally probable. The approximation error introduced by these estimates will be numerically evaluated in Section V, by comparing them with exact results from the model in Section IV-B. Secondly, we will also compare the approximation in [9] to a scalable approach that does not make any assumptions about  $\mu_1^+(i, j, e, t)$ , by considering an imprecise MC whose set of transition rate matrices  $\mathcal{Q}$  contains all the transition rate matrices  $Q$  that are compatible with (13).

When a type 1 requests arrives and finds an available type 1 superchannel (i.e.,  $R := m_1 - i - jn_2 > 0$ ), the following two transitions can occur:  $(i, j, e) \rightarrow (i + 1, j, e - 1)$  or  $(i, j, e) \rightarrow (i + 1, j, e)$ , the rates of which are equal to  $\lambda_P$  and  $\lambda_1 - \lambda_P$ , respectively, where  $\lambda_P$  depends on the state  $(i, j, e)$  and the implemented spectrum allocation policy P. For an arbitrary spectrum allocation policy P, all we can say for sure is that

$$\lambda_P(i, j, e) \in \begin{cases} \{\lambda_1\} & \text{if } i = n_2(m_2 - j - e), \\ \{0\} & \text{if } e = 0, \\ [0, \lambda_1] & \text{otherwise.} \end{cases} \quad (14)$$

For the random allocation policy, we have that  $\lambda_{RA} = \lambda_1^{(en_2)/(m_1 - i - jn_2)}$ , whereas for the other two policies that are considered in this paper, we have that  $\lambda_{LF} = \lambda_{MF} = \lambda_1$  if  $i = (m_2 - j - e)n_2$  and  $\lambda_{LF} = \lambda_{MF} = 0$  if  $i < (m_2 - j - e)n_2$ . We will compare these three policies against an approach that does not make any assumptions about the policy P, by considering an imprecise MC whose set of transition rate matrices  $\mathcal{Q}$  contains all the transition rate matrices  $Q$  that are compatible with (14).

On the one hand, for each of the spectrum assignment policies RA, LF and MF, the approximation for  $\mu_1^+$  in [9] leads to a unique transition rate matrix  $Q$ , and therefore to a unique MC that can furthermore be shown to be ergodic. In this way, for every event  $A \subseteq \mathcal{X}$ , each of these policies leads to a unique approximate limit probability  $\pi_A$ , which can be computed using the methods in Section III-A. On the other hand, by considering the set  $\mathcal{Q}$  of all transition rate matrices that are compatible with (13) and (14), we obtain an imprecise MC. This imprecise MC can also be shown to be ergodic, and therefore, for every  $A \subseteq \mathcal{X}$ , it determines unique lower and upper limit probabilities  $\underline{\pi}_A$  and  $\overline{\pi}_A$ , which can be computed using the methods in Section III-C. In these computations, evaluating Equation (12) is linear in the number of states—hence  $\mathcal{O}(m_1 m_2^2)$ —because, for every state  $x \in \mathcal{X}$ , Fig. 3 implies that  $[Qf](x)$  is a linear function with at most six non-zero coefficients, which we need to minimise with respect to the simple inclusions in (13) and (14). The resulting bounds  $\underline{\pi}_A$  and  $\overline{\pi}_A$  do not require any approximation, nor do they require us to specify a spectrum assignment policy. For all of the above (precise and imprecise) MCs, the approximate and

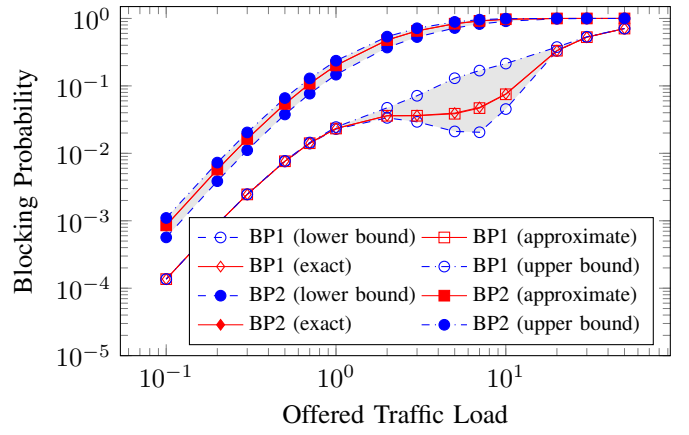


Fig. 4: Blocking probability for a system with  $S = 45$  slices and  $n_2 = 5$ . Random Assignment policy.

lower/upper limit blocking probability BP1 (respectively BP2) experienced by type 1 (respectively type 2) traffic requests corresponds to choosing  $A = \{(i, j, e) \in \mathcal{X} : R = 0\}$  (respectively  $A = \{(i, j, e) \in \mathcal{X} : e = 0\}$ ).

## V. NUMERICAL ASSESSMENT

We consider the spectrum assignment problem over a link with an available spectrum  $T$ , subdivided in slices of  $F = 12.5$  GHz, for a total number of  $S = T/F$  slices. Type 1 superchannels are formed by  $n_1 = 3$  contiguous slices (including guardbands), whereas type 2 superchannels consist of  $n_1 \times n_2 = 3n_2$  slices, where  $n_2$  varies according to the considered scenario. In each scenario, the offered traffic load,  $\rho$ , varies in the range  $0.1 \leq \rho \leq 50$ , we assume  $\rho = \lambda_1/\mu_1 = \lambda_2/\mu_2$  and we set  $\mu_1 = \mu_2 = 1$ .

### A. Comparison to Exact Markov Chains

The exact MC has a large number of states. Therefore it can be solved only for small instances. Fig. 4 shows the blocking probability for type 1, BP1, and type 2, BP2, connections for a system having  $T = 562.5$  GHz,  $S = 45$  slices,  $n_2 = 5$  and a RA policy. The blocking probabilities calculated with the exact MC and with the approximate MC are almost overlapping, providing empirical evidence that the approximations used to reduce the number of states are very good in the case of the RA policy. Additionally, Fig. 4 shows the bounds obtained with an imprecise MC, which models a system with an unspecified assignment policy. In case of type 2 connections, these bounds are close for any traffic load, showing that changing the policy could provide some improvement, but that the RA policy already yields reasonably good performance. In case of type 1 connections, the bounds are very tight for low loads and for high loads, showing that the assignment policy has no impact on the performance. On the other hand, in the central region, for a traffic load  $2 \leq \rho \leq 10$ , where the blocking probability has non-monotonic behaviour, the bounds become looser, suggesting that the policy might have a significant impact on the performance. Also in this case, the RA policy settles halfway between the upper and lower bounds.

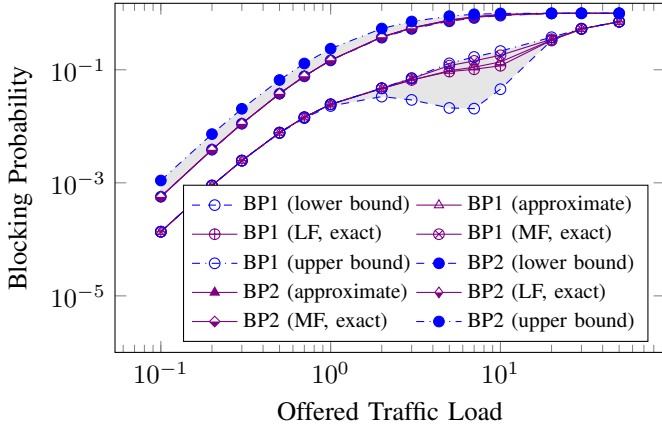


Fig. 5: Blocking probabilities for a system with  $S = 45$  slices and  $n_2 = 5$ . Least Filled (LF) and Most Filled (MF) policies.

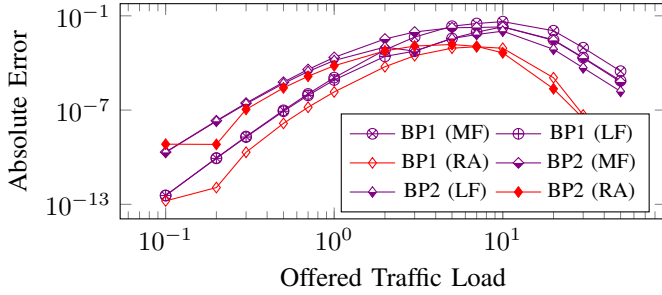


Fig. 6: Absolute error of the blocking probabilities BP1 and BP2 calculated using the approximate Markov chain for the various assignment policies.

Fig. 5 shows the blocking probabilities BP1 and BP2 for a system having  $S = 45$  slices,  $n_2 = 5$  and with either the LF or the MF assignment policy. These two policies have a different performance, which can be evaluated with the respective exact MCs. On the other hand, the approximate model yields an identical approximate MC for the two policies. The figure also reports the bounds obtained with an imprecise MC, which are identical to those reported in Fig. 4. The blocking probability for type 2 connections calculated for the two policies either with the exact model or with the approximate one are overlapping and also very near to the lower bound, suggesting that the LF and MF policies treat these connections in a similar way, also resulting in the best achievable performance. Conversely, the blocking probabilities for the type 1 connections are slightly different for the two policies, with the LF policy performing slightly better. This difference is captured by the exact models, while the approximate model yields results between the two. Additionally, both policies are much nearer to the upper bound than the RA policy, suggesting that the better treatment of type 2 connections results in a worse treatment of type 1 connections.

Fig. 6 shows the absolute error between the blocking probabilities calculated with the exact model and the same probabilities calculated with the approximate MC. All the models are accurate for a low traffic regime and for both

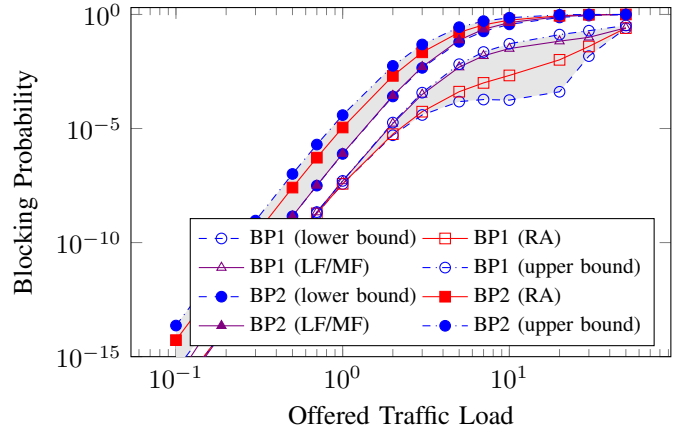


Fig. 7: Blocking probabilities for a system with  $S = 120$  slices and  $n_2 = 4$

blocking probabilities. Since the blocking probability for type 1 connections is lower than the blocking probability for type 2 connections, the absolute error is also lower. As the load grows, the error of the model becomes larger, with the MF and LF model being less accurate than the model for the random assignment for all blocking probabilities, and with the maximum of 0.043 obtained for BP1 (MF) at  $\rho = 10$ . At high load, the error drops for all the policies, with the RA policy dropping much faster. While the accuracy of the approximate MC for the RA policy was already shown by the authors of [9] by means of numerical simulations, we show that the approximation holds well also for the other policies, though with a lesser accuracy. It is also worth noting that the error for the LF and for the MF policies is similar. Therefore, the approximate MC is a good approximation of both policies, being slightly better for LF. This result was also seen in Fig. 5.

### B. Application to Large Systems

Fig. 7 shows the blocking probabilities for a large system with  $T = 1.5$  THz,  $S = 120$  slices and  $n_2 = 4$ . For each connection type, the figure shows the performance of the RA policy and of the MF/LF policies, all obtained with the approximate MC. In addition, the same figure shows the bounds for an unspecified policy. For the type 2 connections, the large bounds suggest that the policy has an impact on the performance. In fact, the MF and LF policies are very close to the lower bound, confirming that these policies are among the best ones for type 2 connections, whereas the RA policy is situated more or less in the middle of the two bounds. On the other hand, the blocking probabilities for type 1 connections show that the performance of the MF and LF policies is very close to the upper bound. Similarly to the small case discussed above, the bounds for type 1 connections are closer for small traffic and larger for medium traffic.

Fig. 8 shows the blocking probabilities for a large system with  $S = 120$  slices and  $n_2 = 20$ . As before, the figure shows, for each of the two connection types, the performance of our three policies—again for the approximate MC—and the bounds for an unspecified policy. For the type 2 connections,

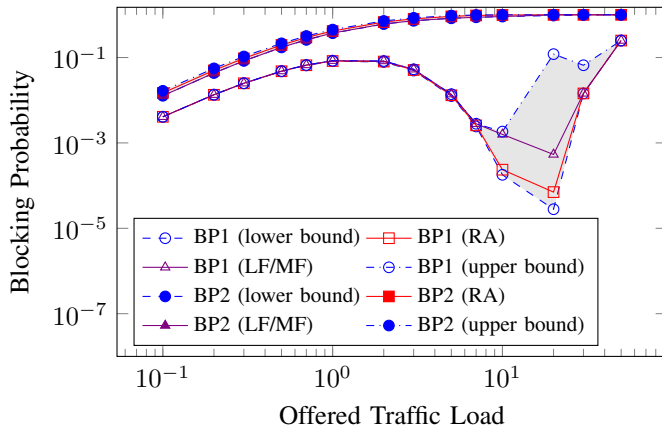


Fig. 8: Blocking probability for a system with  $S = 120$  slices and  $n_2 = 20$

the LF/MF policies again lie along the lower bound and the RA policy is in the middle. Conversely, the blocking probabilities for type 1 connections have tight bounds for low traffic and loose bounds for medium to high traffic. The probabilities calculated for the RA and LF/MF policies are very similar except in the region where  $10 \leq \rho \leq 20$ , in which the LF/MF policies always have a larger blocking probability than the RA policy and are in some cases very close to the upper bound.

## VI. CONCLUSION

We have studied the problem of spectrum assignment in a two-service flexi-grid optical link. First, we provided exact Markov chain models for the cases of random, most-filled, and least-filled assignment policies. The complexity of these models is exponential in the number of slices though, so they do not scale. Therefore, next, we evaluated an approximate, reduced-state Markov chain model that is available in the literature for a random assignment policy, and extended it to the case of the most-filled and least-filled policies. The comparison to the exact results in a small scale case shows that the approximation is good, but it is difficult to obtain an evaluation of its precision for large scale problems. For this reason, finally, we introduced a Markov model that uses imprecise probabilities. This model scales to large problems and does not make assumptions about the assignment policy, making it possible to provide guaranteed bounds on the achievable blocking probabilities. This new model can be used for two different purposes: to evaluate the precision of an approximate Markov model in large scale problems, and to provide policy-free performance bounds.

## REFERENCES

- [1] O. Gerstel, M. Jinno, A. Lord, and S. B. Yoo, "Elastic optical networking: A new dawn for the optical layer?" *IEEE Commun. Mag.*, vol. 50, no. 2, pp. s12–s20, 2012.
- [2] *Spectral grids for WDM applications: DWDM frequency grid*, ITU Telecommunication Standardization Sector Recommendation ITU-T G.694.1, Feb. 2012. [Online]. Available: <http://www.itu.int/>
- [3] M. Jinno, H. Takara, B. Kozicki, Y. Tsukishima, Y. Sone, and S. Matsuoka, "Spectrum-efficient and scalable elastic optical path network: architecture, benefits, and enabling technologies," *IEEE Commun. Mag.*, vol. 47, no. 11, pp. 66–73, 2009.
- [4] M. D. Feuer and S. L. Woodward, "Advanced ROADMs networks," in *National Fiber Optic Engineers Conference*. Optical Society of America, 2012, paper NW3F.3.
- [5] Y. Yin, Z. Zhu, S. B. Yoo *et al.*, "Fragmentation-aware routing, modulation and spectrum assignment algorithms in elastic optical networks," in *Optical Fiber Communication Conference*. Optical Society of America, 2013, paper OW3A.5.
- [6] Y. Yu, J. Zhang, Y. Zhao, X. Cao, X. Lin, and W. Gu, "The first single-link exact model for performance analysis of flexible grid WDM networks," in *National Fiber Optic Engineers Conference*. Optical Society of America, 2013, paper JW2A.68.
- [7] Z. Shen, H. Hasegawa, K. Sato, T. Tanaka, and A. Hirano, "A novel elastic optical path network that utilizes bitrate-specific anchored frequency slot arrangement," *Optics express*, vol. 22, no. 3, pp. 3169–3179, 2014.
- [8] J. Comellas and G. Junyent, "On the worthiness of flexible grid in elastic optical networks," in *41st European Conference on Optical Communication (ECOC'15)*. IEEE, Sep. 2015, pp. 1–3.
- [9] J. Kim, S. Yan, A. Fumagalli, E. Oki, and N. Yamanaka, "An analytical model of spectrum fragmentation in a two-service elastic optical link," in *2015 IEEE Global Communications Conference (GLOBECOM'15)*. IEEE, Dec. 2015, pp. 1–6.
- [10] —, "Two-service analytical model for partially-shared elastic optical link spectrum," in *2016 IEEE 17th International Conference on High Performance Switching and Routing (HPSR'16)*. IEEE, Jun. 2016, pp. 75–80.
- [11] P. Walley, *Statistical reasoning with imprecise probabilities*. Chapman and Hall, 1991.
- [12] T. Augustin, F. P. Coolen, G. de Cooman, and M. C. Troffaes, Eds., *Introduction to Imprecise Probabilities*, ser. Wiley Series in Probability and Statistics. Wiley, 2014.
- [13] G. Zhang, M. De Leenheer, A. Morea, and B. Mukherjee, "A survey on OFDM-based elastic core optical networking," *IEEE Commun. Surveys Tuts.*, vol. 15, no. 1, pp. 65–87, 2013.
- [14] I. Tomkos, E. Palkopoulou, and M. Angelou, "A survey of recent developments on flexible/elastic optical networking," in *14th International Conference on Transparent Optical Networks (ICTON'12)*. IEEE, Jul. 2012, pp. 1–6.
- [15] S. Azodolmolky, M. Klinkowski, E. Marin, D. Careglio, J. S. Pareta, and I. Tomkos, "A survey on physical layer impairments aware routing and wavelength assignment algorithms in optical networks," *Computer Networks*, vol. 53, no. 7, pp. 926–944, 2009.
- [16] Z. Shen, H. Hasegawa, and K. Sato, "A novel flexible grid/semi-flexible grid optical path network design algorithm that reserves exclusive frequency slots for high bitrate signals," in *18th International Conference on Optical Network Design and Modeling (ONDM'14)*, May 2014, pp. 287–292.
- [17] J. Kim, X. Wang, S. WangYan, M. Razo, M. Tacca, and A. Fumagalli, "Blocking fairness in two-service EONs with uneven arrival rates," in *17th International Conference on Transparent Optical Networks (ICTON'15)*, Jul. 2015, pp. 1–4.
- [18] X. Wang, J. Kim, S. Yan, M. Razo, M. Tacca, and A. Fumagalli, "Blocking probability and fairness in two-rate elastic optical networks," in *16th International Conference on Transparent Optical Networks (ICTON'14)*, Jul. 2014, pp. 1–4.
- [19] D. Škulj, "Efficient computation of the bounds of continuous time imprecise markov chains," *Applied Mathematics and Computation*, vol. 250, pp. 165–180, Jan. 2015.
- [20] T. Krak, J. De Bock, and A. Siebes, "Imprecise continuous-time markov chains," 2016, submitted.
- [21] M. C. Troffaes, J. Gledhill, D. Škulj, and S. Blake, "Using imprecise continuous time markov chains for assessing the reliability of power networks with common cause failure and non-immediate repair," in *Proc. of the 9th International Symposium on Imprecise Probability: Theories and Applications (ISIPTA'15)*, Jul. 2015, pp. 287–294.
- [22] D. Škulj and R. Hable, "Coefficients of ergodicity for markov chains with uncertain parameters," *Metrika*, vol. 76, no. 1, pp. 107–133, 2013.
- [23] S. Lopatzidis, J. De Bock, G. de Cooman, S. De Vuyst, and J. Walraevens, "Robust queueing theory: an initial study using imprecise probabilities," *Queueing Systems*, vol. 82, no. 1, pp. 75–101, Feb. 2016.
- [24] J. De Bock, "The limit behaviour of imprecise continuous-time markov chains," *Journal of Nonlinear Science*, pp. 1–38, 2016.